

Kinetic analysis of sucrose activated carbon for nutrient removal in water

Sara Jamaliniya^a, O. D. Basu^{IWA^{a,*}}, Saumya Suresh^a, Eustina Musvoto^b
and Alexis Mackintosh^c

^a Department of Civil and Environmental Engineering, Carleton University, 1125 Colonel By Drive, Ottawa, ON, Canada K1S 5B6

^b TruSense Engineering, 887 Northern Way, Vancouver, BC, Canada

^c PCS Technologies Inc., #204-3800 Westbrook Mall, Vancouver, BC, Canada V6S2L9

*Corresponding author. E-mail: onita.basu@carleton.ca

Abstract

A renewable, green activated carbon made from sucrose (sugar) was compared with traditional bituminous coal-based granular activated carbon (GAC). Single and multi-component competitive adsorption of nitrate and phosphate from water was investigated. Langmuir and Freundlich isotherm models were fitted to data obtained from the nitrate and phosphate adsorption experiments. Nitrate adsorption fits closely to either Freundlich or Langmuir model for sucrose activated carbon (SAC) and GAC with a Langmuir adsorption capacity of 7.98 and 6.38 mg/g, respectively. However, phosphate adsorption on SAC and GAC demonstrated a selective fit with the Langmuir model with an adsorption capacity of 1.71 and 2.07 mg/g, respectively. Kinetic analysis demonstrated that adsorption of nitrate and phosphate follow pseudo-second-order kinetics with rate constant values of 0.061 and 0.063 g/(mg h), respectively. Competitive studies between nitrate and phosphate were demonstrated in preferential nitrate removal with GAC and preferential phosphate removal with SAC. Furthermore, nitrate and phosphate removals decreased from 75% removal to 35% removal when subject to multi-component solutions, which highlights the need for adsorption analysis in complex systems. Overall, SAC proved to be competitive with GAC in the removal of inorganic contaminants and may represent a green alternative to coal-based activated carbon.

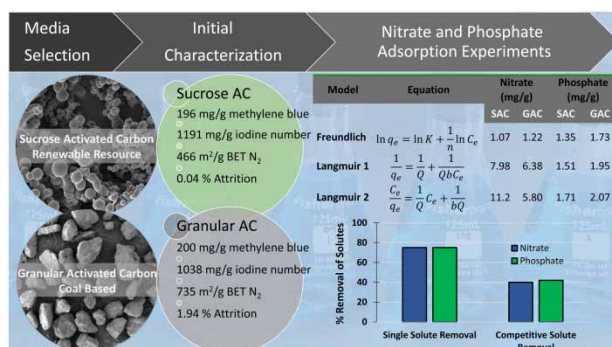
Key words: activated carbon, adsorption, green adsorbent, multi-component, nitrate, phosphate

Highlights

- Nitrate and phosphate were similarly removed by the produced green adsorbent compared to a typical GAC.
- Competitive adsorption decreased removals of nitrate and phosphate by 50%.
- Iodine number for the green adsorbent was found to be 1,191 mg/g.
- Kinetic data followed pseudo-second-order kinetics.
- The green adsorbent was determined to be competitively comparable to coal-based GAC.

This is an Open Access article distributed under the terms of the Creative Commons Attribution Licence (CC BY 4.0), which permits copying, adaptation and redistribution, provided the original work is properly cited (<http://creativecommons.org/licenses/by/4.0/>).

Graphical Abstract



INTRODUCTION

Inorganic nutrients in industrial and municipal wastewater effluents commonly contain phosphates, nitrate, nitrite, ammonia and potentially heavy metals which contaminate surrounding water streams. Phosphate and nitrogen species are known to be the main causes for eutrophication of water bodies. For instance, phosphate levels over 0.02 mg/L lead to algal blooms which, in turn, leads to loss of species, loss of habitat, increased turbidity and reduced visibility of water (Huang *et al.* 2009; Kilpimaa *et al.* 2015). Municipal wastewater (before treatment) typically contains 4–15 mg/L of phosphorus, while industrial wastewater may contain phosphate levels over 10 mg/L (Mezener & Bensmaili 2009). Ammonia and nitrate also contribute to nitrification. Nitrification is a two-step microbiological process which consists of oxidizing ammonia to nitrite followed by nitrite oxidation to nitrate. In drinking water treatment, nitrification can impact chloramine levels during secondary disinfection practices. Losses in chloramine level due to the nitrification is measured by increases in nitrate levels (Berry *et al.* 2006). Systems experiencing nitrification could potentially have increased the concentration of nitrite and nitrate, which are regulated contaminants (Wilczak *et al.* 1996). Furthermore, high nitrate concentration in drinking water can cause methemoglobinemia (blue baby syndrome), stomach cancer, colorectal cancer and non-Hodgkin's lymphoma. The USEPA maximum recommended concentration of nitrate in drinking water is 10 mg/L (EPA 2019).

Various physical, chemical and biological techniques have been applied in order to remove phosphate and nitrate from water including ion exchange, electro-coagulation, chemical precipitation, microbial uptake and conversion as well as adsorption (de-Bashan & Bashan 2004). Adsorption is one popular option due to ease of implementation and capacity to treat a broad range of nitrate and phosphate concentrations in water. Adsorption efficiency highly depends on the adsorbent used for the given adsorbate. Granular activated carbon (GAC) is one of the most commonly used adsorbents for various contaminants because of its versatility, high adsorption capacity, ease of operation and maintenance, high surface area and pore volume (Kilpimaa *et al.* 2015). However, GAC is commonly obtained from fossil fuels such as bituminous coal which can contribute to climate change. Zero waste strategies to use green adsorbents are an aspect as society focuses on sustainable development. Utilizing generated waste for more beneficial purposes reduces waste disposal and may provide alternative sources for activated carbon. Research in this field of utilizing raw and/or waste materials with high carbon content has been studied for adsorption of phosphorus and nitrate from water such as coconut husk, agricultural residues, macadamia nutshells and coffee endocarp (Kilpimaa *et al.* 2015). The nitrate adsorption capacity from various other green activated sources has been reported in other research such as 1.24 mg/g with coconut AC (Liu *et al.* 2018), 1.1 mg/g for wheat straw charcoal and 1.30 mg/g for mustard straw charcoal (Mishra & Patel 2009). The phosphate adsorption capacity was reported to be 7.3–7.7 mg/g for coir pith activated carbon (Kumar *et al.* 2010) and

10.6 mg/g for iron hydroxide-eggshell waste (Mezenner & Bensmaili 2009). Furthermore, currently, most research on nitrate and phosphate removal has focussed on single contaminant removal from water (Huang *et al.* 2009; Cho *et al.* 2011; Ragheb 2013; Liu *et al.* 2018). However, in practice, these contaminants will be present together along with several other competing contaminants in water. Therefore, multi-component water studies are required to aid in an improved understanding of phosphate and nitrate adsorptive removal in the environment.

Although research has been ongoing for the development of an activated carbon adsorbent from sustainable, and/or waste resources, with high carbon content, the research in this field is still young and in need of further exploration (Satayeva *et al.* 2018). One potential renewable carbon source is sucrose which can be obtained from household, agricultural and food-based industrial wastes. Research, however, is lacking in sucrose activated carbon (SAC) for the removal of inorganic contaminants such as nitrate and phosphate (Santoso *et al.* 2020).

Thus, this research examines the novel potential of using sucrose as a green activated carbon adsorbent for removal of inorganic nitrate and phosphate in a multi-component solution. The research objectives are to assess the adsorption isotherms and kinetic models of SAC with various nitrate and phosphate solutions in two types of water systems.

EXPERIMENTAL

Adsorbents

An initial characterization study was completed to assess different traits for the SAC and GAC materials. SAC was obtained by hydrothermal carbonization of organic material sucrose followed by pyrolysis activation at 900 °C. Brunauer–Emmett–Teller (BET) specific surface area analysis was performed by an N₂ adsorption test at CANMET, Canada. Particle size analysis was carried out using ImageJ™ from the scanning electron microscopy (SEM) image of the media. The attrition percentage was determined by suspending approximately 1 g of the adsorbent in 100 ml of 0.07 M sodium acetate–0.03 M acetic acid buffer. The mixture was left on a stirrer for 24 h. This mixture was then washed with distilled water on 50 mesh sieve and the retained carbon was transferred to an aluminum pan and heated to 105 °C for 2 h, allowed to cool and the final weight was noted. The attrition percentage is the weight difference of the adsorbent before and after the treatment divided by the initial weight of the adsorbent (Toles *et al.* 2000). The experimentally determined attrition values of SAC were lower than that of GAC. Attrition values are important in fluidized column treatment processes where intraparticle abrasion leads to media degradation with adverse impacts on operating life. Bulk densities were analyzed as per ASTM D2854-96.

Iodine adsorption studies were carried out according to ASTM D 4607-94 (2006). Three sets of masses of the two media samples were taken and mixed with 100 ml of 0.100 ± 0.001 N standard iodine solution, after 30 s of equilibrium time the solution was filtered, and 50 ml of filtrate was used to determine residual iodine concentration by titration with standard sodium thiosulfate with starch as the indicator. Methylene blue number, a standard parameter to quantify adsorption capacity which represents the mesopore and macropore capacity of adsorbents, was determined to establish if SAC and GAC had comparable initial adsorption properties (Hameed *et al.* 2007; Raposo *et al.* 2009). Methylene blue adsorption experiments were carried out by agitating different masses of SAC and GAC suspended in 5 mg/L solution of methylene blue dye in Erlenmeyer flasks at 50 rpm, 21 ± 3 °C in a rotary shaker (New Brunswick Excella E-1 Open Air Shaker). Residual dye concentration was sampled and measured using a UV-Visible spectrophotometer (Spectronic Unicam) by measuring the absorbance at 650 nm.

Adsorbates – experimental solutions

SAC and GAC were used for adsorption equilibrium and kinetic studies. Four different solutions were studied at room temperature to evaluate the adsorption performance of the SAC and GAC with the various nitrate and phosphate solutions. Solutions (I) and (II) were single solute solutions of nitrate and phosphate prepared in milli-Q water. Solutions (III) and (IV) were multi-component solutions, with (III) prepared in milli-Q water, while solution (IV) was a synthetic raw water containing carbon, nitrogen and phosphate sources. The solutions are listed in Table 1.

Table 1 | Nitrate and phosphate experimented solutions, temperature 20 °C

Solution	Component	Concentration (mg/L)	Source chemicals	pH ^a
(I) Single component	Nitrate	2.0	Potassium nitrate	5–6
(II) Single component	Phosphate	2.0	Potassium dihydrogen phosphate	5–6
(III) Two components (N : P ratio 1 : 1)	Nitrate	2.0	Potassium nitrate	5–6
	Phosphate	2.0	Potassium dihydrogen phosphate	
(IV) Synthetic raw water (C : N : P ratio: 25 : 5 : 1)	Carbon	20	Glyoxal, formic acid and acetic acid	7–7.5
	Nitrogen	4.0	Potassium nitrate	
	Phosphorus	0.80	Potassium dihydrogen phosphate	
	Alkalinity	25–50	Calcium carbonate	

^aSolutions I, II and III were prepared in milli-Q water with an unadjusted pH of 5–6, IV was prepared in milli-Q water with a pH of 7–7.5.

Batch equilibrium studies

Adsorption experiments were carried out by agitating different masses of SAC and GAC suspended in 2 mg/L NO₃⁻ solution of potassium nitrate for nitrate adsorption studies and 2 mg/L PO₄³⁻ solution of potassium dihydrogen phosphate for phosphate adsorption studies in an Erlenmeyer flask at 50 rpm, 21 ± 3 °C in a rotary shaker (New Brunswick Excella E-1 Open Air Shaker). The pH of the solution was maintained in the 7–8 range by the addition of sodium hydroxide and/or hydrochloric acid solution. The concentration of nitrate and phosphate in solution was investigated using a UV-Visible spectrophotometer (Spectronic Unicam) by measuring the absorbance at 345 and 660 nm, respectively. Preliminary testing was conducted to determine equilibrium time for each sample after which batch adsorption tests were conducted. The equilibrium time was determined to be between 100 and 220 h for the various samples. The absorbance of the solutions in contact with both media was then measured to determine residual concentration. All analysis was conducted as duplicates. Langmuir and Freundlich isotherms were then fitted to data to study the adsorption capacity of the two media for each adsorbate. The competitive adsorption studies were carried out by subjecting SAC and GAC to multi-component solutions (II), (III) and (IV) with the composition noted in Table 1.

The most commonly studied adsorption models, Freundlich and Langmuir, were analyzed in this study.

Freundlich isotherm is applied to adsorption data for nitrate and phosphate adsorption on SAC and GAC as follows:

$$\log(q_e) = \log k_f + \left(\frac{1}{n}\right) \log C_e \quad (1)$$

where q_e is the amount of adsorbate adsorbed per mass of the adsorbent used (mg/g), C_e is the equilibrium concentration of the adsorbate in solution (mg/L), k_f (mg/g) and n are the constants

representing the adsorption capacity and intensity of adsorption. Freundlich is an empirical model which suggests heterogeneity of adsorption sites attributed to non-uniform distribution of energy sites for adsorption and that adsorption is not limited to single-layer formation on the adsorbent (Foo & Hameed 2010). The plot of $\log q_e$ versus $\log C_e$ gives a straight line and the k_f and n parameters were calculated from the intercept and slope of the plots, respectively, for SAC and GAC.

The Langmuir isotherm model represented by the following equations was also applied to the adsorption of nitrate and phosphate on SAC and GAC. Two different linearization forms of Langmuir isotherm were studied including Langmuir 1, Langmuir 2 represented by Equations (4) and (5), respectively:

$$\frac{1}{q_e} = \left(\frac{1}{bQ_0} \right) \times \frac{1}{C_e} + \frac{1}{Q_0} \quad (2)$$

$$\frac{C_e}{q_e} = \frac{1}{Q_0 b} + \frac{C_e}{Q_0} \quad (3)$$

where C_e is the concentration of adsorbate in solution (mg/L) at equilibrium. The constant Q_0 signifies the adsorption capacity (mg/g) and b is related to the energy of adsorption (L/mg). The linear analysis using different linear forms of the Langmuir equation will provide a different possibility to parameter estimation (Ho 2006). It should also be noted that Equation (4) is extremely sensitive to variability at low values of q_e and it may lead to clumping of data points near origin and Equation (5) presents C_e and q_e as combined and dependent terms which may result in an overestimation of each parameter. However, the ease with which linearized Langmuir equations can be fit to data has led to accepting the fitted model parameters as representative of the adsorbent (Bolster & Hornberger 2007). Therefore, in this study, data were plotted to two different forms of Langmuir isotherms.

Batch kinetics studies

Kinetic studies were carried out by subjecting SAC and GAC media to test solutions in Erlenmeyer flasks agitated on a rotary shaker (New Brunswick Excella E-1 Open Air Shaker) at 50 rpm, 21 ± 3 °C. For this study, the preliminary adsorption experiments at adsorbent dosages of 0.24, 0.48, 0.64 and 0.96 g/L were carried out. Solution samples were withdrawn at predetermined time intervals to determine residual nitrate and phosphate concentrations. The amount of adsorption q_t (mg/g) at a given time (t) is calculated by:

$$q_t = \frac{(C_0 - C_t) \times V}{W} \quad (4)$$

where C_0 and C_t (mg/L) are the liquid-phase concentrations of nitrate and phosphate at initial and predetermined times, t , respectively. V is the volume of the solution (L) and W is the mass of dry adsorbent used (g). Preliminary kinetic studies for adsorption of nitrate and phosphate on SAC and GAC were carried out for different adsorbent dosages of 0.24, 0.48, 0.64 and 0.96 g/L to observe the range over which kinetic studies are feasible and not limited by masses. Experimentally, higher errors were obtained at the lower dosages, and thus, a dosage of 0.96 g/L was selected for the kinetic studies.

Several kinetic models are used to evaluate the experimental data for examining the controlling mechanisms of adsorption processes such as mass transfer and chemical reaction (Öztürk & Bektas 2004). In this study, three kinetics models were investigated to define the mechanism of adsorption and potential rate-controlling steps such as chemical reaction, diffusion control and mass transport processes. Pseudo-first-order, pseudo-second-order and intraparticle diffusion

models were used to analyze the experimental data to determine which one can best describe the adsorption reactions. The pseudo-first-order reaction considers a linear relationship between the sorption rate and the adsorption capacity, while the second-pseudo-order reactions assume that the rate-limiting step is the interaction between two reagent particles. The controlling mechanism in the intraparticle diffusion kinetic model is diffusion where the rate of adsorption process is dependent on the diffusion speed of the adsorbate to the adsorbent (Mazarji *et al.* 2017).

The pseudo-first-order model is expressed by the Lagergren equation:

$$\log(q_e - q_t) = \log(q_e) - \frac{k_1 t}{2.303} \quad (5)$$

where q_e and q_t (mg/g) are the amount of adsorbate adsorbed onto the sorbent at equilibrium and time t with k_1 the pseudo-first-order rate constant (min^{-1}). The plot of $\log(q_e - q_t)$ versus t for the data gives linear relationship which was used to find the values of k_1 and q_e from the slope and intercept, respectively.

The pseudo-second-order model is expressed by the following equation to analyze second-order kinetics of nitrate and phosphate adsorption on SAC and GAC:

$$\frac{t}{q_t} = \frac{1}{k_2 q_e^2} + \frac{t}{q_e} \quad (6)$$

where q_e is the amount of adsorbate adsorbed per unit mass of sorbent at equilibrium (mg/g), q_t is the amount of adsorbate adsorbed (mg/g) at contact time t and k_2 is the pseudo-second-order rate constant (g/mg min). The linear plot of t/q_t versus t gives the values of q_e and k_2 which can be determined from the slope and the intercept, respectively.

The intraparticle diffusion model is expressed by the following equation. Intraparticle diffusion is studied to confirm if the rate-limiting step is the diffusion of nitrate and phosphate across the adsorbents:

$$q_t = k_d t^{1/2} + C \quad (7)$$

where q_t is the amount of adsorbate adsorbed (mg/g) at contact time t and k_d is the intraparticle diffusion rate constant ($\text{mg/g min}^{1/2}$) and C describes the thickness of boundary layer (mg/g).

The mean square error (MSE) test method was used to evaluate best fit of the adsorption isotherm model to the experimental data using Equation (8), wherein a lower MSE value corresponds to a decreased error and represents a better curve fit. Where n is the number of data points, q_{ecal} is the calculation from the models and q_e is the observation from experiments (Fatih 2013):

$$\text{MSE} = \frac{1}{n} \sum_{i=1}^n (q_{\text{ecal}} - q_e)^2 \quad (8)$$

RESULTS AND DISCUSSION

Initial characterization study

The initial characterization study is discussed in this section to assess different traits for the SAC and GAC materials. The physical properties of the SAC and GAC are presented in Table 3 and SEM images of both media are shown in Figure 1. The virgin SAC (Figure 1(a)) is comprised of spherical

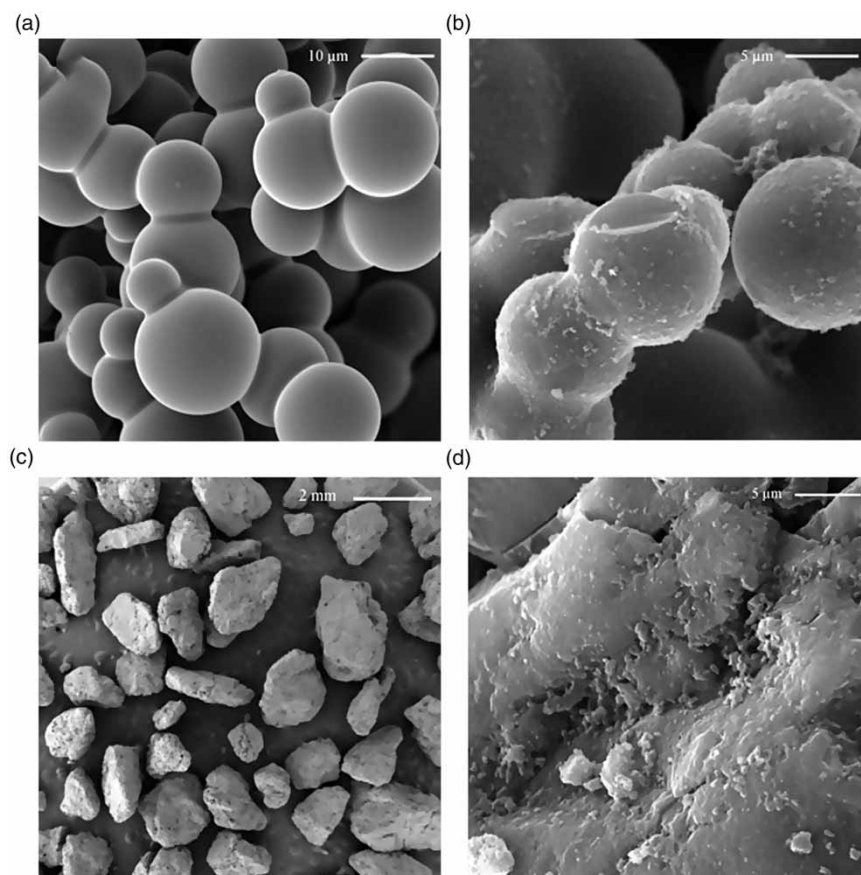


Figure 1 | SEM images of adsorbents: (a) virgin SAC media, (b) SAC with adsorbed methylene blue, (c) virgin GAC media and (d) GAC with adsorbed methylene blue.

particles with smooth surfaces, whereas the virgin GAC (Figure 1(c)) has particles with a more porous and rougher surface. BET surface area analysis based on N₂ adsorption indicates that the SAC had a lower surface area compared to the GAC at 466 ± 7 versus $735 \text{ mg}^2/\text{g}$, respectively. Imaging analysis further allowed for media size comparison with calculated average particle diameter size ranges of the media as 2.96–9.68 and 420–840 μm for the SAC versus GAC, respectively. The SAC material was made through a novel processing technology and thus likely may need some further research to increase particle size.

Methylene blue and iodine numbers were determined in the initial characterization study. Methylene blue is considered as a model compound for removal of organic compounds and colored contaminants from aqueous solutions because of its strong adsorption onto solids and is, thus, used as a standard for describing a new media. In this study, SAC and GAC were determined to have similar adsorption capacities for methylene blue dye with values of 196 and 200 mg/g , respectively. Figure 1(b) and 1(d) show the methylene blue dye adsorbed to the respective media surface.

Meanwhile, iodine adsorption capacity defines the capacity of activated carbon materials to adsorb smaller particles. The iodine number for SAC and GAC was found to be similar, although the SAC iodine adsorption was found to be slightly higher than GAC, as presented in Table 2. Iodine number is often used as a representation of the available surface area for attachment, thus although the BET value for GAC was greater than the SAC; the iodine number suggests that the SAC and GAC useful adsorption capacities are similar. Overall, the initial characterization study supports the hypothesis that SAC may be competitive to GAC for adsorption processes.

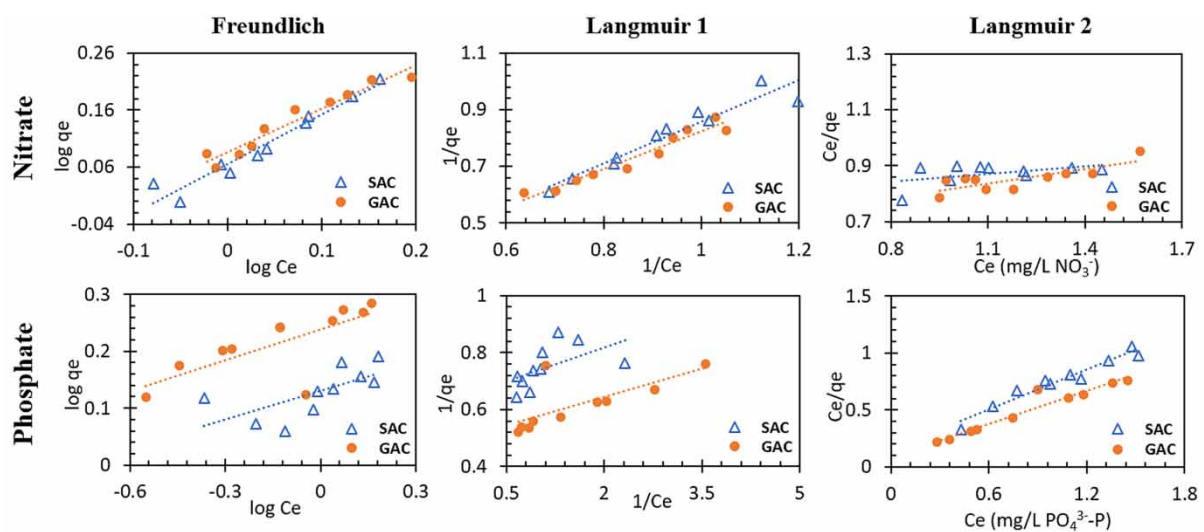
Table 2 | Physical characterizations of SAC and GAC

Properties	SAC	GAC
Particle size (μm)	2.96–9.68 ^a	420–840 ^b
Surface area (BET N ₂) (m^2/g)	466 \pm 7 ^a	735 ^b
Bulk density (g/cm^3)	0.40 ^a	0.51 ^a
Ash content (%)	0.1 ^a	12 ^b
pH of adsorbent	5.96 ^a	5.79 ^a
Moisture content (%)	1.9 ^a	2 ^b
Attrition (%)	0.04 ^a	1.94 ^a
Iodine number (mg/g)	1,191 ^a	1,038 ^b
Methylene blue number (mg/g)	196 ^a	200 ^a

^aExperimentally determined.^bManufacturer provided.

Adsorption studies

Adsorption isotherm studies were conducted to determine the maximum adsorption capacities of SAC and GAC for nitrate and phosphate adsorbates to assess for side-by-side comparisons of a novel green activated carbon produced in this research to a commercially purchased GAC. The values of Q_0 and b for SAC and GAC were calculated from the slope and the intercept, respectively, of the linear plots (Figure 2). The correlation coefficients for the Freundlich model ($R^2 = 0.95$ and 0.94) (Figure 2) were slightly higher compared to Langmuir models 1 and 2, indicating that the Freundlich isotherm demonstrates a better fit for adsorption of nitrate on SAC and GAC, respectively. This suggests that nitrate adsorption on activated carbon is heterogeneous. The values obtained for $1/n$ are 0.87 and 0.76 for SAC and GAC, respectively, indicating that nitrate is favorably adsorbed onto both the adsorbent surfaces under study as they are in the range $0 < 1/n < 1$. The k_f values for nitrate adsorption on SAC and GAC are 1.16 and 1.22 ($\text{mg}/\text{g}(\text{L}/\text{mg})^{1/n}$), respectively. Even though the Freundlich k_f value gives a measure of relative adsorption capacity, it does not directly give the adsorption capacity. Several authors have compared various Langmuir models for adsorption capacity (Ho 2006; Bolster & Hornberger 2007). In this research, the adsorption capacity was additionally fitted to both

**Figure 2** | Adsorption isotherm models and adsorption capacity K (Freundlich) and Q (Langmuir) of SAC and GAC in solutions (I) and (II), respectively.

Langmuir 1 and Langmuir 2 (refer to Table 3); the Langmuir 1 model yielded a significantly higher correlation coefficient compared to Langmuir 2 (0.92–0.94 versus 0.22–0.64) as a measure of nitrate adsorption capacity. In general, Langmuir adsorption capacity has been the more typically reported adsorption capacity value in different studies and the low MSE values for Langmuir isotherm confirms that it is a good fit for adsorption of nitrate onto SAC and GAC. Therefore, the Langmuir adsorption capacity of nitrate is 7.98 and 6.38 mg/g for SAC and GAC, respectively.

Table 3 | Adsorption isotherm models and adsorption capacities for single solute nitrate and phosphate solutions

Isotherm	Equation and R^2	Adsorption parameter (mg/g)	Nitrate		Phosphate	
			SAC	GAC	SAC	GAC
Freundlich	$\ln q_e = \ln K + \frac{1}{n} \ln C_e$	K	1.16	1.22	1.35	1.73
	R^2		0.95	0.94	0.45	0.57
	MSE		1.60×10^{-05}	1.81×10^{-05}	8.22×10^{-05}	1.77×10^{-02}
Langmuir 1	$\frac{1}{q_e} = \frac{1}{Q} + \frac{1}{QbC_e}$	Q	7.98	6.38	1.52	1.95
	R^2		0.92	0.94	0.35	0.52
	MSE		1.63×10^{-05}	1.70×10^{-05}	0.21	1.93×10^{-02}
Langmuir 2	$\frac{C_e}{q_e} = \frac{1}{Q} C_e + \frac{1}{bQ}$	Q	11.3	5.80	1.71	2.07
	R^2		0.22	0.64	0.94	0.93
	MSE		1.64×10^{-05}	1.64×10^{-05}	0.01	2.03×10^{-02}

The Langmuir adsorption capacity for SAC for nitrate obtained is higher than the values obtained in the literature for the adsorption capacity of nitrate by other green adsorbents. Mizuta *et al.* (2004) reported 1.25 mg/g Langmuir adsorption capacity for bamboo powder charcoal for nitrate and 1.7 mg/g for coconut activated carbon (Mizuta *et al.* 2004; Bhatnagara & Sillanpää 2011).

Compared to nitrate, phosphate adsorption appears to follow Langmuir isotherm better than Freundlich. The MSE value is smaller than 1, indicating that Langmuir isotherm is a good fit in this adsorption process. This can potentially represent monolayer adsorption of phosphate onto homogenous adsorption sites on both SAC and GAC. The pH of the adsorbent's surface was found to be in the 4–6 range which suggests the presence of protonated OH⁻ ions on acidic media. This supports the adsorption of the negatively charged phosphate group on the adsorbent surface. Analytical studies as part of future studies will help to determine the type of adsorbate–adsorbent interaction (Tran *et al.* 2017).

However, the q_e values for SAC and GAC are 1.71 and 2.07 mg/g which indicates that the SAC has a slightly lower adsorption capacity to remove phosphate than that of GAC. The adsorption capacities of SAC and GAC for removing nitrate and phosphate using the three isotherm models are presented in Table 3.

Kinetic studies

The adsorption data obtained for the removal of nitrate and phosphate by SAC and GAC over the equilibrium time period were applied to all three kinetic models and the data obtained are presented in Table 4. For each adsorbate based on regression of coefficient analysis and based on the lower degree of difference between the calculated and experimental q_e values, the pseudo-second-order model showed best fit for both nitrate and phosphate removal by SAC and GAC compared to pseudo-first-order and intraparticle diffusion model. The pseudo-second-order model fit for both adsorbates. This could potentially indicate that the rate-limiting step in the process may be chemisorption of nitrate and phosphate on activated carbons which involves valence exchange via sharing or

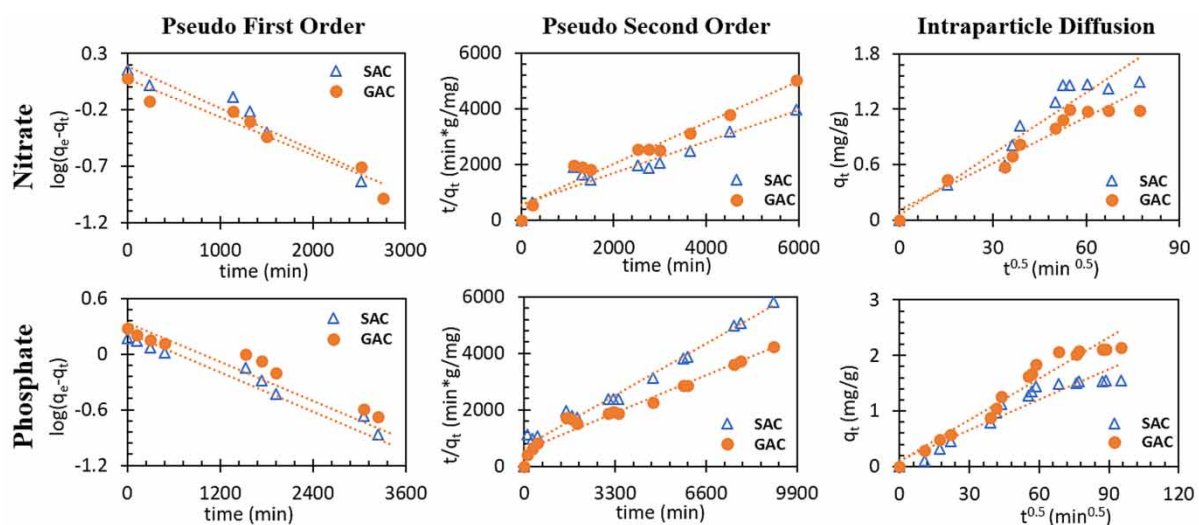
Table 4 | Kinetic models parameters for nitrate and phosphate in solutions (I) and (II)

Model	Equation	Parameters	Unit	Nitrate		Phosphate	
				SAC	GAC	SAC	GAC
Pseudo-first-order	$\log(q_e - q_t) = \log(q_e) - (k_1 t / 2.303)$	q_e	mg/g	1.01	1.21	1.19	1.42
		q_t	mg/g	1.27	1.17	1.74	1.48
		k_1	h ⁻¹	0.07	0.04	0.08	0.05
		R^2		0.96	0.94	0.82	0.55
Pseudo-second-order	$\frac{t}{q_t} = \frac{1}{k_2 q_e^2} + \frac{t}{q_e}$	q_t	mg/g	1.35	1.34	1.19	1.40
		k_2	g/mg h	0.07	0.06	0.06	0.06
		R^2		0.98	0.95	0.95	0.96
Intraparticle diffusion	$q_t = K_d t^{1/2} + C$	q_t	mg/g	0.14	0.6	0.08	0.43
		K_d	g/mg min ^{1/2}	1.73×10^{-02}	0.02	0.01	3.00×10^{-06}
		R^2		0.88	0.65	0.93	0.73

exchange of electrons (Duman *et al.* 2003). However, as shown by Tran *et al.* (2017), several additional analytical techniques, for example, NMR, XRD, XPS and CHN elemental analysis, need to be performed to confirm chemisorption.

This agrees with other studies which found nitrate and phosphate adsorption depends more on surface chemistry than structural properties (Nunell *et al.* 2015).

The pseudo-second-order rate constant k_2 for nitrate and phosphate removal, as presented in Table 4, are comparatively similar making SAC as fast as GAC in the adsorption process of both nitrate and phosphate. Intraparticle diffusion plot for both nitrate and phosphate did not pass through the origin and does not give a straight line, indicating that the rate-limiting step in the process is not intraparticle diffusion (Figure 3). The adsorption of nitrate and phosphate involves initial instantaneous adsorption on the external surface of both SAC and GAC followed by diffusion into the spaces between particles and pores that generates a difference in layer thickness over both the adsorbents which is given by the intercept from intraparticle diffusion plot for SAC as 0.14 mg/g and for GAC as 0.60 mg/g for nitrate and 0.08 mg/g SAC and 0.43 mg/g GAC for phosphate adsorption. The kinetic studies conclude that adsorption of nitrate and phosphate on SAC and GAC follow initial pseudo-second-order adsorption on the surface. Further, analytical studies will confirm whether there is a transition of adsorption through slow diffusion into intraparticle space in SAC and pores in GAC (Tran *et al.* 2017).

**Figure 3** | Kinetic model fits of nitrate and phosphate in solutions (I) and (II).

The measured surface area provides an opportunity to compare the experimental adsorption capacities of GAC and SAC. As shown in Table 4, the phosphate adsorption capacities of GAC was slightly higher than SAC. However, adsorption capacity can also be considered by the available area of the material relative to the mass removed. Thus, by dividing the adsorption capacities by BET (m^2/g) of GAC and SAC, it was determined that the amount of each adsorbate adsorbed per surface area of adsorbent is higher onto SAC (refer to Table 5). This is noteworthy as the produced SAC (as observed in the SEM images) has a smooth surface, indicating that surface adsorption dominates, meanwhile GAC has both the exterior surface and interior surface area available for adsorption.

Table 5 | Adsorption capacity of SAC and GAC for removing nitrate and phosphate

	Unit	Nitrate		Phosphate	
		SAC	GAC	SAC	GAC
Adsorption capacity ^a	mg/g	7.98	6.38	1.71	2.07
Adsorption capacity	mg/m ²	0.0171	0.0087	0.0037	0.0028

^aBased on Langmuir isotherm.

Multi-component competitive solution study

Multi-component competitive adsorbent studies were conducted in two different solution systems (Solutions III and IV). Nitrate and phosphate removal in single-component solution by SAC and GAC show high removal of these contaminants with removal percentages of 70% and above. However, the removal percentage for these contaminants drops when they present in a solution with other contaminants which reflect on more realistic scenarios in water treatment. The nitrate removal decreases to 40% from 75% by SAC when present in solution III and to 33% in solution IV. Similarly, phosphate removal decreases from 75% by SAC in single-component solution to 42% in solution III and to 36% in solution IV system. Solution III with the nitrate and phosphate contaminants in milli-Q water show higher phosphate removal by SAC and higher nitrate removal by GAC (Table 6). Thus, it appears as though nitrate adsorption is preferable with more porous media GAC. The same observations for phosphate removal and nitrate removal occur with solution II. It was observed that nitrate removal percentage in solution (IV) was 17 and 28% lower onto SAC and onto GAC, respectively, as compared to the adsorption of nitrate in solution (III). Similarly, the adsorption of phosphate is 15 and 16% lower in solution (IV) than that of solution (III) onto SAC and GAC, respectively, therefore, suggesting that the adsorption of nitrate and phosphate is depressed by other competing components in the solution (Manjunath & Kumar 2018).

Table 6 | Single and competitive adsorption removal of nitrate and phosphate for SAC and GAC

Solution	Media	Nitrate		Phosphate	
		Removal (%)	Equilibrium time (h)	Removal (%)	Equilibrium time (h)
Solution (I)	SAC	75	100	n/a	
	GAC	81	100		
Solution (II)	SAC	n/a		75	100
	GAC			77	100
Solution (III)	SAC	39.7	105	42.2	220
	GAC	51.5	105	40.8	200
Solution (IV)	SAC	33	220	35.8	200
	GAC	36.8	200	34.3	220

Adsorbent dosage of 0.96 g/L was used.

Furthermore, the time for equilibrium increased as the complexity of the solution increased (i.e. single-component milli-Q water to multi-component with synthetic raw water). It is shown in Figure 4 that the adsorption significantly reached equilibrium in the single solutions with a higher rate of removal, while in the other two multi-component solutions, not only the equilibrium took place slower but also the removal is not as significant as the simple solutions. Thus, this research clearly highlights the need for multi-component complex raw waters to be studied more or to recommend pilot tests for adsorption studies to ensure adequate results on adsorption capacity.

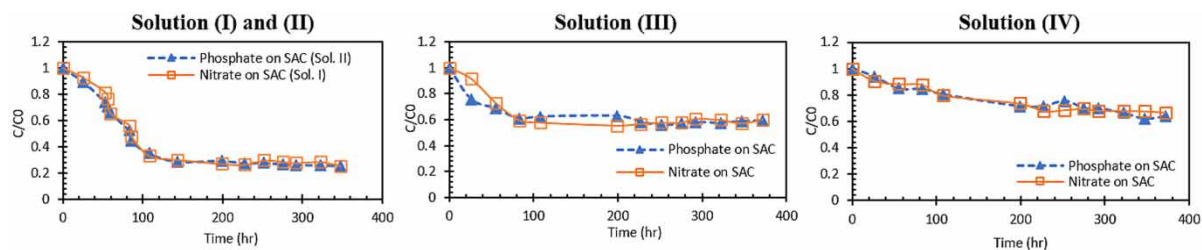


Figure 4 | C/C_0 versus time for solutions I-IV, showing increasing times for removal and decreased removals as solution complexity increases.

CONCLUSION

The experimental results suggest that SAC can be used as a viable green alternative for GAC in the removal of phosphate and nitrate from water. The adsorption data for removal of nitrate by SAC demonstrates that it fits reasonably well with the Freundlich and Langmuir 1 isotherms with a Langmuir adsorption capacity of 7.98 mg/g and for phosphate removal, it fits Langmuir 2 isotherm with an adsorption capacity of 1.71 mg/g which are both competitively comparable to GAC (6.38 and 2.07 mg/g, respectively). Competitive adsorption studies with multiple contaminants in water show large reductions in the amount of nitrate and phosphate removed from solution by SAC and GAC and highlight the need for studies with more complex solutions. Kinetic modeling shows nitrate and phosphate removal fit pseudo-second-order with similar rates of adsorption for both the adsorbates on SAC and GAC supports the potential to use SAC as a green adsorbent in water treatment processes.

Financial modeling including CAPEX and OPEX costs associated with using SAC as a replacement for GAC needs to be performed to analyze the cost-effectiveness of using alternative media. Cost analyses and pilot-scale studies using SAC in adsorption columns will be the focus of the future studies.

ACKNOWLEDGEMENTS

This research was made possible by funding from NSERC. Extending thanks to Nano Imaging Facility, Carleton University and CANMET, Ottawa, Canada, for analytical assistance with the SEM and BET analysis. Also extending gratitude to Dr Glenn McRae, Dr Marie Tudoret and Chamathka Varushawithana, Carleton University, Ottawa, Ontario, for their help.

DATA AVAILABILITY STATEMENT

All relevant data are included in the paper or its Supplementary Information.

REFERENCES

- Berry, D., Xi, C. & Raskin, L. 2006 Microbial ecology of drinking water distribution systems. *Environmental Biotechnology* **17**, 297–302.
- Bhatnagara, A. & Sillanpää, M. 2011 A review of emerging adsorbents for nitrate removal from water. *Chemical Engineering Journal* **168**, 493–504.
- Bolster, C. H. & Hornberger, G. 2007 On the use of linearized Langmuir equations. *Nutrient Management, Soil and Plant Analysis* **71** (6), 1796–1806.
- Cho, D.-W., Chon, C.-M., Kim, Y., Jeon, B.-H., Schwartz, F. W., Lee, E.-S. & Song, H. 2011 Adsorption of nitrate and Cr(VI) by cationic polymer-modified granular activated carbon. *Chemical Engineering Journal* **175**, 298–305.
- de-Bashan, L. E. & Bashan, Y. 2004 Recent advances in removing phosphorus from wastewater and its future use as fertilizer (1997–2003). *Water Research* **38**, 4222–4246.
- Duman, A., Aygun, S. & Yenisoay-Karakas, I. 2003 Production of granular activated carbon from fruit stones and nutshells and evaluation of their physical, chemical and adsorption properties. *Microporous and Mesoporous Materials* **66**, 189–195.
- EPA 2019 National Primary Drinking Water Regulation Report Number EPA 816-F-09-004, s.l.: s.n.
- Fatih, D. 2013 Adsorption properties of low-cost biomaterial derived 455 from *Prunus amygdalus* L. for dye removal from water. *The Scientific World Journal* **2013**, 8. <https://doi.org/10.1155/2013/961671>.
- Foo, K. & Hameed, B. 2010 Insights into the modeling of adsorption isotherm systems. *Chemical Engineering Journal* **156**, 2–10.
- Hameed, B., Din, A. & Ahmad, A. 2007 Adsorption of methylene blue onto bamboo-based activated carbon: kinetics and equilibrium studies. *Journal of Hazardous Materials* **141**, 819–825.
- Ho, Y.-S. 2006 Isotherms for the sorption of lead onto peat: comparison of linear and non-linear methods. *Journal of Environmental Studies* **15** (1), 81–86.
- Huang, X., Liao, X. & Shi, B. 2009 Adsorption removal of phosphate in industrial wastewater by using metal-loaded skin split waste. *Journal of Hazardous Materials* **166**, 1261–1265.
- Kilpimaa, S., Runtti, H., Kangas, T., Lassi, U. & Kuokkanen, T. 2015 Physical activation of carbon residue from biomass gasification: novel sorbent for the removal of phosphates and nitrates from aqueous solution. *Journal of Industrial and Engineering Chemistry* **21**, 1354–1364.
- Kumar, P., Sudha, S., Chand, S. & Srivastava, V. C. 2010 Phosphate removal from aqueous solution using coir-pith activated carbon. *Separation Science and Technology* **45**(10), 1463–1470.
- Liu, L., Ji, M. & Wang, F. 2018 Adsorption of nitrate onto ZnCl₂-modified coconut granular activated carbon: kinetics, characteristics, and adsorption dynamics. *Advances in Materials Science and Engineering* **2018**, 12. <https://doi.org/10.1155/2018/1939032>.
- Manjunath, S. & Kumar, M. 2018 Evaluation of single-component and multi-component adsorption of metronidazole, phosphate and nitrate on activated carbon from *Prosopis juliflora*. *Chemical Engineering Journal* **346**, 525–534.
- Mazarji, M., Aminzadeh, B., Baghdadi, M. & Bhatnagar, A. 2017 Removal of nitrate from aqueous solution using modified granular activated carbon. *Journal of Molecular Liquids* **233**, 139–148.
- Mezener, N. Y. & Bensmaili, A. 2009 Kinetics and thermodynamic study of phosphate adsorption on iron hydroxide-eggshell waste. *Chemical Engineering Journal* **147**, 87–96.
- Mishra, P. & Patel, R. 2009 Use of agricultural waste for the removal of nitrate-nitrogen from aqueous medium. *Journal of Environmental Management* **90**, 519–522.
- Mizuta, K., Matsumoto, T., Hatate, Y., Nishihara, K. & Nakanishi, T. 2004 Removal of nitrate-nitrogen from drinking water using bamboo powder charcoal. *Bioresource Technology* **95**, 255–257.
- Nunell, G., Fernandez, M., Bonell, P. & Cukierman, A. 2015 Nitrate uptake improvement by modified activated carbons developed from two species of pine cones. *Journal of Colloid and Interface Science* **440**, 102–108.
- Öztürk, N. & Bektas, T. E. 2004 Nitrate removal from aqueous solution by adsorption onto various materials. *Journal of Hazardous Materials* **B112**, 155–162.
- Ragheb, S. M. 2013 Phosphate removal from aqueous solution using slag and fly ash. *Housing and Building National Research Center Journal* **9**, 270–275.
- Raposo, F., Rubia, M. D. L. & Borja, R. 2009 Methylene blue number as useful indicator to evaluate the adsorptive capacity of granular activated carbon in batch mode: influence of adsorbate/adsorbent mass ratio and particle size. *Journal of Hazardous Materials* **165**, 291–299.
- Santoso, E., Ediati, R., Kusumawati, Y., Bahruji, H., Sulistiono, D. O. & Prasetyoko, D. 2020 Review on recent advances of carbon based adsorbent for methylene blue removal from waste water. *Materials Today Chemistry* **16**, 100233.
- Satayeva, A. R., Howell, C. A., Korobeinyk, A. V., Jandosov, J., Inglezakis, V. J., Mansurov, Z. A. & Mikhalovsky, S. V. 2018 Investigation of rice husk derived activated carbon for removal of nitrate contamination from water. *Science of The Total Environment* **630**, 1237–1245.
- Toles, C. A., Marshall, W. E., Johns, M. M., Wartelle, L. H. & McAloon, A. 2000 Acid-activated carbons from almond shells: physical, chemical and adsorptive properties and estimated cost of production. *Bioresource Technology* **71**, 87–92.
- Tran, H. N., You, S.-J., Hosseini-Bandegharaei, A. & Chao, H.-P. 2017 Mistakes and inconsistencies regarding adsorption of contaminants from aqueous solutions: a critical review. *Water Research* **120**, 88–116.
- Wilczak, A., Jacangelo, J. G., Marcinko, J. P., Odell, L. H. & Kirmeyer, G. J. 1996 Occurrence of nitrification in chloraminated distribution systems. *American Water Works Association* **88** (7), 74–85.

First received 6 February 2020; accepted in revised form 15 June 2020. Available online 14 July 2020